Digital Signal Processing Simulations for a 2-D Ultrasonic Array System

Luis G. ULLATE, Oscar MARTÍNEZ, Montserrat PARRILLA, CSIC, Madrid, Spain
Ovidiu VERMESAN, L-C. BLYSTAD, SINTEF, Oslo, Norway
Benoit FROELICH, Kenneth LIANG, Schlumberger, Clamart, France

Abstract. A new ultrasonic system based on a 2-D cylindrical array with capability of electronic scanning and 3D beam-forming was developed. Such a system can operate in harsh environments for casing inspection (diameter, ovality, corrosion, thickness, cracks) and for assessment of the material behind casing. The most important challenges of such a system are:
(a) operation in highly attenuative media (up to 12 dB/cm/MHz) with ambient conditions of up to 175ºC and 1400 bar,
(b) the large number of array elements (N=800) and the volume restrictions for the array electronics (around 1000cm^3), which requires a high level of integration.

The system operates in a frequency band that corresponds to the fundamental thickness resonance of the casing (200 – 700 kHz). Using Sigma Delta modulators (SDM) for mixed signal processing facilitates integration and reduces the number of interconnections.
It is well known that increasing the oversampling ratio (OSR) of SDM increases the dynamic range of the signals. The system is limited by the maximum sampling frequency that together with the input frequency of up to 1 MHz defines the OSR. In the paper we present the digital processing algorithms for casing measurements based on the response of an ideal plate, and make a theoretical analysis of the effect of several parameters of the digital processing chain on the casing measurements. We conclude that, in the presence of noise, the averaging effect of the array beamforming greatly improves the measurements, allowing the use of SDM with relatively low OSRs.

Introduction

A new ultrasonic system based on a 2-D cylindrical array with capability of electronic scanning and 3D beam-forming has been developed. As the primary objective of this new ultrasonic imaging system is to perform non destructive testing in fluid filled oil wells, it has to operate in harsh environments for casing inspection (diameter, ovality, corrosion, thickness, cracks) and for assessment of the material behind casing (a cement annulus is typically used to provide mechanical support for the casing string, but more importantly to provide zonal hydraulic isolation). Although the system was optimised for oil-field application, the concept can be used in other applications such as: fluid distribution (gas, water, oil), manufacturing plants, subsea pipelines, nuclear plants, etc. Such ultrasonic system based on a 2D cylindrical array has several advantages:

- Electronic scanning eliminates the need for a mechanical rotating motor drive, which could stall out in heavy mud due to viscous drag.
- Electronic beam-forming enables in-situ reconfiguration of the beam pattern to suit multiple measurement needs and to adjust to changing bore-hole geometry without a costly trip to surface to replace the transducer.

- Electronic beam-forming allows real-time optimization of imaging performance to reduce the effect of tool position eccentering and/or non-circular borehole cross-section.
- The system is expandable and has built-in versatility to accommodate new measurement techniques.

The borehole environment imposes severe restrictions on the system. Down-hole pressure and temperature often reach extremes of 1400 bar and 175° C. Borehole fluids are typically loaded with mineral particles to achieve a range of densities from 1000 $kg.m^{-3}$ to 2000 $kg.m^{-3}$ and beyond, which results in a wide range of fluid acoustic impedances and velocities, and also leads to progressively higher ultrasonic attenuation (up to 12dB/cm/MHz [1]). This attenuation severely limits the maximum usable frequency to around 500 kHz, which is near the resonance frequency of the tube thickness. The principle of measurements is similar to the existing ultrasonic techniques [2,3]: the transducer emits a short pulse which excites a resonance mode in the casing. The analysis of the echo gives four measurements: diameter of the tube, rugosity, casing thickness and cement acoustic impedance.

The most important challenge of the ultrasonic system is due to the large number of array elements (800 elements in our prototype) and the limited volume and its form factor available for the electronics (around $1000cm^3$), what calls for a high degree of integration and a special packaging configuration. In this sense, using sigma delta (SD) modulators for analog to digital (AD) conversion facilitates integration and, as it gives the results in a single bit, it drastically reduces the interconnections. It is well known that increasing the oversampling ratio (OSR) of SD modulation increases the dynamic range of the signals [4,5]. However, the power consumption is directly proportional to the sampling frequency, and due to the high borehole temperature (up to 175ºC) the system is limited by the maximum sampling frequency that together with the input frequency of up to 1 MHz defines the OSR.

In this paper, the problem of finding the design parameters of the ultrasonic system based on SD conversion is studied. The simulations are based on the ideal response of a plate presented in [2]. We also make a theoretical analysis of the effect of several parameters of the digital processing chain (including the sampling frequency) and analyse the influence of noise on the casing measurements.

Principles of simulations

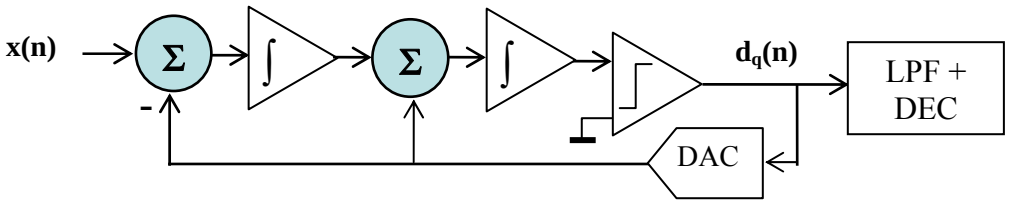

Figure 1: Schematic of a second order Δ–Σ modulator

1.1 SD conversion

SD modulation is an efficient means of transforming an analog voltage into a digital representation for several reasons. On the one hand, the single-bit digital output simplifies the interconnections of the array electronics. This fact is more important for 2D array systems because they typically involve digital processing of hundreds of channels for

beamforming in reception. On the other hand, SD modulators use simple, standard-precission analog circuitries operating at very high speed to attain high OSR and to achieve sufficient signal to quantization noise ratio. Consequently, these components are easy to integrate together with other analog or digital circuits on a single chip, in contrast with conventional multibit AD converters, which require high precision analog circuits that are difficult to integrate.

SD modulators use one or more integration stages (order of the SD modulator) within a feedback path as shown in Figure 1: the difference between the quantizer output $d_1(n)$ and the modulator input x(n) (quantization error) accumulates in the integrator until it swings the quantizer in the other direction. The quantization noise (SQNR) produced by a DS modulator mainly depends on its order and on the sampling frequency (f_S). The oversampling ratio (OSR) is [4,5]:

$$OSR=f_S/2f_B,$$

f_B being the upper signal band-edge. A first evaluation of the dynamic range due to the quantization noise [4] can be done for a continuous wave input to a first order SDM, doubling the oversampling ratio reduces the noise power by 9dB. Higher order SDMs provide even better signal to noise ratio. For example, a 2^{nd} order SDM improves SQNR by 15 dB for every doubling of the sampling frequency. Therefore, for OSR=8, the SQNR is approximately 45dB for narrow band pulses (this means that using pulses of 0.65 MHz and 100% bandwidth, the sampling frequency f_S must be close to 16MHz). However, DS modulators of order higher than 2 are prone to instabilities.

The modulator output is a sequence of high-low voltage levels which indicates 1 and -1 for the beamforming algorithms. Reconstruction of multibit signals requires a low pass filter (LPF) which cuts off quantization noise above the signal band. This filter must be carefully designed to reject this noise and prevent it from aliasing into the signal band upon decimation. After the signal is sufficiently filtered it is often decimated (DEC) to reduce the data rate of downstream processing components.

1.2 Plate impulse response

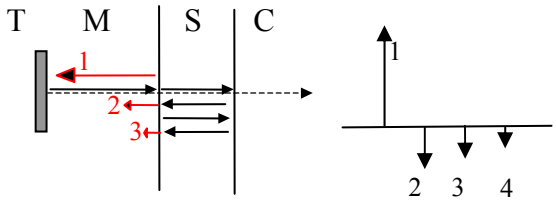

Figure2: Impulse response of a plate

The principle of measurements is the following: a subaperture of the 2D cylindrical array emits a wide-band pulse at normal incidence to the casing surface, which excites thickness resonance in the casing. The echo from the casing is received by the sub-aperture elements and beam-formed (this is digitally converted, properly delayed for eccentering correction and summed). As the tube is thin and its diameter is large compared to the pulse wavelength, the problem can be approximated by a flat 2D array emitting waves onto a flat plate of the same thickness. This approximation reduces the resonance problem to the impulse response of a plate (as it is shown in Figure 2), which is formed by a simple sequence of Dirac delta pulses.

We consider three propagation media: (a) mud M, whose acoustic impedance Z_M can vary between 1.5 and 3 Mrayl depending on the mud composition, (b) steel S with Z_S=46 Mrayl and (c) cement C, with Z_C varying from 1.5 to approximately 6 Mrayl.

The first interface mud-steel gives rise to the first reflected echo. Part of the energy is transmitted into the plate, and propagates to the second interface steel-cement where a new process reflection-transmission occurs (Figure 2). Thus, for an incident impulse, the reflected pulse consists of an initial reflection P1 of high amplitude, followed by a decaying series of inverted impulses whose amplitudes depend on the acoustic impedances of the mud, steel and cement, and are given by the following expressions:

$$P_1 = \frac{Z_S - Z_M}{Z_S + Z_M} \quad (1)$$

$$K_R = \frac{P_2}{P_1} = \frac{4Z_S Z_M (Z_C - Z_S)}{(Z_S - Z_M)(Z_C + Z_S)(Z_S + Z_M)} \quad (2)$$

P_1 and P_2 indicating the amplitudes of the first and second pulses, respectively. The amplitude decay for the subsequent pulses is also given by:

$$K_A = \frac{P_3}{P_2} = \frac{P_{N+1}}{P_N} = \frac{(Z_C - Z_S)(Z_M - Z_S)}{(Z_C + Z_S)(Z_M + Z_S)} \quad (3)$$

From Equation (3), it is obvious that amplitude decay rate is higher as the mud and cement acoustic impedances increase closer to that of steel. After many reflections on the cement interface, the amplitude becomes very small (i.e. -50dB after 10 reflections), and, therefore, also the signal to noise ratio. For this reason, digital processing analysis is best weighted mostly on the early part of the echo signal (6-7 reflections maximum) where there is higher signal to noise ratio.

The time of arrival of the initial reflection is

$$t_1 = 2d/v_M, \quad (4)$$

where d is the distance from the transducer to the plate and v_M is the sound velocity in the mud. The time separation of the train of negative pulses is equal to the round-trip propagation time within the steel plate:

$$\Delta t = 2e/v_S \quad (5)$$

where e is the thickness of the plate and v_S is the sound velocity in the steel.

In the upper part of Figure 3 the echo from a plate calculated by the convolution of the plate impulse response and a wideband Gaussian pulse whose central frequency f_R has been adjusted to the thickness resonance ($f_C = v_S/2e$), and whose relative bandwidth is 100%. The initial parameters are: Z_M=2Mrayl, Z_S=46Mrayl, Z_C=5Mrayl, v_S =6mm/μs, e=10mm (therefore f_C=300 KHz), and d=80mm. The peak of the spectrum is due to resonance, and can be used for two important measurements: casing thickness and cement impedance.

Attenuation effect:

The wave attenuation during propagation through the mud is:

$$\Delta A(f) = -\alpha_A * 2d * f, \quad (6)$$

where $\Delta A(f)$ is the loss of amplitude in dB at each frequency f, α_A is the attenuation coefficient that can vary from 0 (for water) to 12dB/MHz/cm (for dense oil mud). Thus, attenuation behaves like a low-pass filter applied to the ultrasonic waves spectrum, as it attenuates more of the higher frequency spectral components. This effect causes, besides a loss of amplitude, a change of the signal waveform due to relative increase of low frequency content.

In the lower part of Figure 3, the distortion of the echo pulse can be observed, which is caused by a loss of amplitude in the higher frequencies. For noisy signals, this loss of amplitude can severely affect measurements based on the signal spectrum.

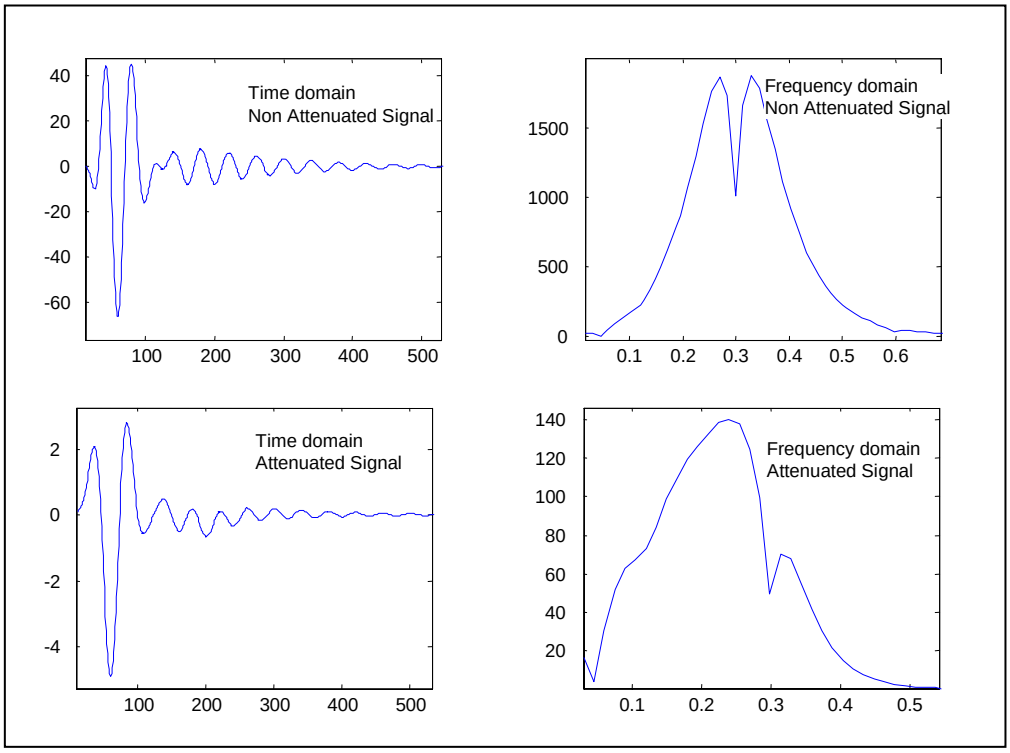

Figure 3: Time (left) and frequency (right) domains of the plate response. Up: non attenuate signal; bottom: signal with 6dB/MHz/cm attenuation. The time of flight until the casing has been omitted in the figure.

1.3 Method for measurements

For the measurements, we shall follow the method based on the casing resonance presented by A.J. Hayman in [2]. The tube internal diameter is measured from the echo position and its roughness is given by the variation of the pulse amplitude. The standoff measurements over one rotation allow the determination of tool eccentering, from which the correction of the beam angle can be computed.

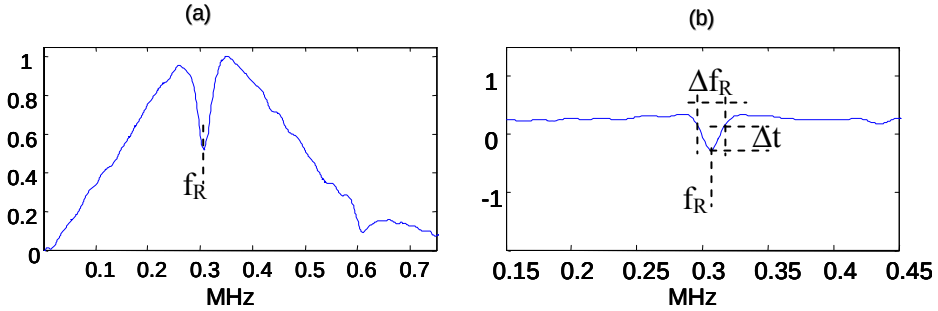

Figure 4: Spectrum amplitude of the echo from the casing resonance (a) and group delay corresponding to the same echo (b)

The measurement of the tube thickness is determined by the position of the resonant frequency f_R in the spectrum (Figure 4-a):

$$e = v_S / 2 f_R \qquad (7)$$

However, such measurement is less susceptible to noise if we take the minimum of the group delay (Figure 4-b), which can be calculated as the derivative of the phase with respect to the angular frequency.

The cement impedance can be also obtained from the group delay curve, as the fractional bandwidth ($\Delta f_R/f_R$) increases as the cement impedance (and therefore the decaying rate of resonance pulses) increases.

Simulations

2.1 Digital signal processing based on SD conversion

In a first stage we have developed simulation tools with the object of analysing the digital signal processing algorithms based on SD conversion. We have considered the signal received by a single transducer when a plane wave impinges on a plate. The different parts related to digital processing are shown in Figure 5:

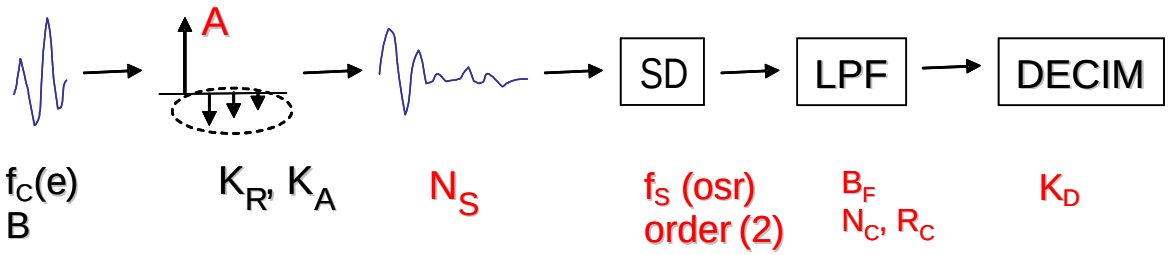

Figure 5. Schema of digital signal processing simulations

- The emitted pulse whose central frequency f_C excites the casing in thickness resonance ($f_C=v_S/2e$). The influence of the off-resonance caused by attenuation and of the signal bandwidth can be analysed.
- The plate impulse response allows making an analysis of the impedance and thickness measurements. The corresponding expressions for the decaying factors K_A and K_R as a function of the acoustic impedances are shown in equations 2 and 3. Changing the amplitude A of the first echo gives information about the dynamic range related to the digital part.
- The number of samples N_S of the received signal is given by the time acquisition window and sampling frequency. N_S must be high enough for receiving at least six resonant echoes from the casing.
- White noise of uniform distribution and programmable amplitude is added to the received signal.
- Two different algorithms have been employed to model a second order SD modulator: (a) the Matlab toolbox from R.Rschreier and (b) the Matlab algorithms from S. Borge (Sintef). Both algorithms give practically equivalent results. From these tools, we have analysed the effect of sampling frequency on the quantization noise.
- In the low pass filter (a Hamming window is considered), we analyse the influence of the number of coefficients and their resolution (4-8 bits or real).
- In addition to the low-pass filter, a time window is applied to the A-scan in order to eliminate the noise content in the zone where the amplitude of the signal is smaller. In this sense, a Hamming window with a width equivalent to 7-9 reflections is recommended [2].
- Finally the effect of different degrees of decimation on the measurement results has been studied.

We have made the corresponding simulations by changing the previous parameters and we obtained the following conclusions:

(a) For OSR ≤ 16, the quantization noise is very high and the group delay measurements are inaccurate even for no-noisy signals.
(b) If we consider noisy signals (white noise with amplitude 10% of the signal peak) the previous problem gets worse, making the SD conversion of single transducers practically unacceptable.
(c) One way of reducing noise is by averaging the signals, and ultrasonic arrays have the advantage that beamforming involves an averaging process. In our simulations we have added white noise to 30 basic signals. Then we have averaged the output of the SD converter before passing to the low-pass filter. Averaging improves random and quantization noise, but the group delay is still not uniform for OSR ≤ 16.
(d) Applying a time window (Hamming) to the signals with a limited width (up to 8 pulse reflections), the group delay becomes soft and uniform even for OSR=16. The application of this time window is of great benefit in the tube measurements.
(e) Increasing the noise content to -12 dB and maintaining 30 averages, the measurements deteriorate slightly. This effect can be improved by increasing the number of averages, what means increasing the number of elements of the 2D array aperture.
(f) For OSR=16, at least 64 coefficients of 8 bits resolution are needed for obtaining good enough results in the FIR low-pass filter.
(g) Decimation of the time-domain signals allows data reduction but still maintains a correct calculation of the measured parameters, with the only condition that the Nyquist criterion is fulfilled.

2.2 Influence of noise and sampling frequency on the measurements

In this part we make an analysis of the error in the measurements due to quantization noise (which is a function of OSR) and white noise added to the signals. These are the calculation stages: from the cement-casing impedances, the impulse response of the plate is first calculated (we consider the following values: e=10mm, v_S=6mm/ms, Z_S=46, Z_C=5, Z_M=2). Later the resonant pulse is calculated by convolution of the plate impulse response with the reference pulse, which is f_C=0.3 MHz of central frequency and 100% of relative bandwidth (f_B≈0.5MHz). Then the signal is digitized at different sampling frequencies and a random noise is added of different levels; an averaging of 30 signals is applied in order to emulate the beamforming process of a 30-elements array aperture, and finally, a low-pass filter (64 coefficients-8bits resolution) is applied to the resulting signal. This process is repeated for 100 times for every noise level and OSR, and the mean value and standard deviation (STD) are calculated in all cases. Figures 6 to 9 show the mean value of each parameter varying OSR from 12 to 25 (this means sampling frequencies from 12MHz to 25 MHz), and the noise level in the signal from -40 dB to -14dB (these values are relative to the signal amplitude). The standard deviation of the simulated measurements is also shown in the graphics.

2.2.1. Amplitude of the main pulse

The amplitude of the main pulse gives a qualitative evaluation of the casing condition. It has been obtained from the peak of the pulse envelope, which has been calculated as the absolute value of the Hilbert transform of the signal. Figure 6 shows this measurement as a fraction of the maximum amplitude accepted by the DS converter.

For OSR=12, the amplitudes are almost horizontal lines only dependent on the sampling frequency (an explanation of these variations can be found on the low-pass filtering used during digital processing, which is different for every sampling frequency, therefore giving different peak amplitude). The standard deviation is however less than 1 % in all cases, what is very satisfactory.

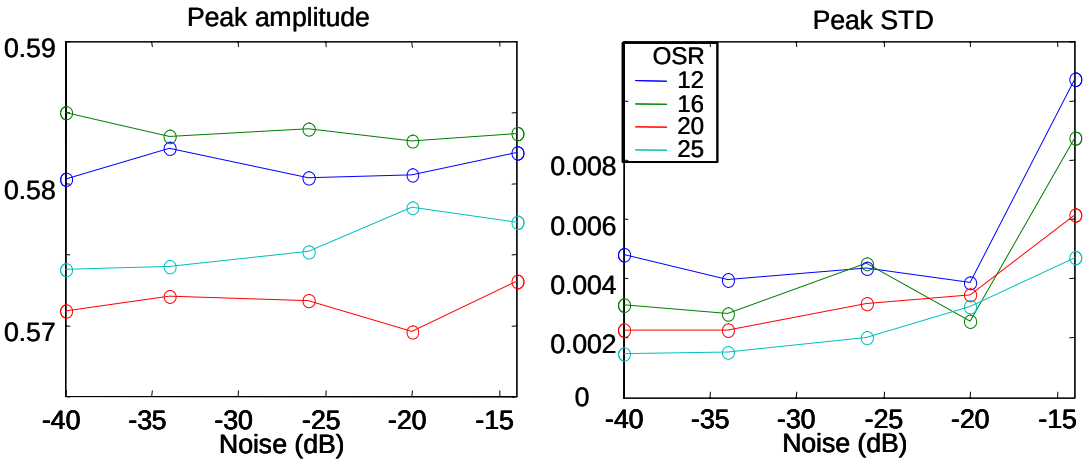

Figure 6: Variation of the signal peak amplitude with respect to noise and oversampling ratio. Right hand: mean value, left hand: standard deviation of 100 measurement simulations

2.2.2. Position of the main pulse

The position of the main pulse is obtained from equation 4, considering the peak of the pulse envelope, which has been calculated by the Hilbert transform. Measurements present variations with the sampling frequency (±10 samples), but they do not change with the noise content. These variations are caused by the low-pass filtering stage used during digital processing, which gives a different time delay for every sampling frequency.

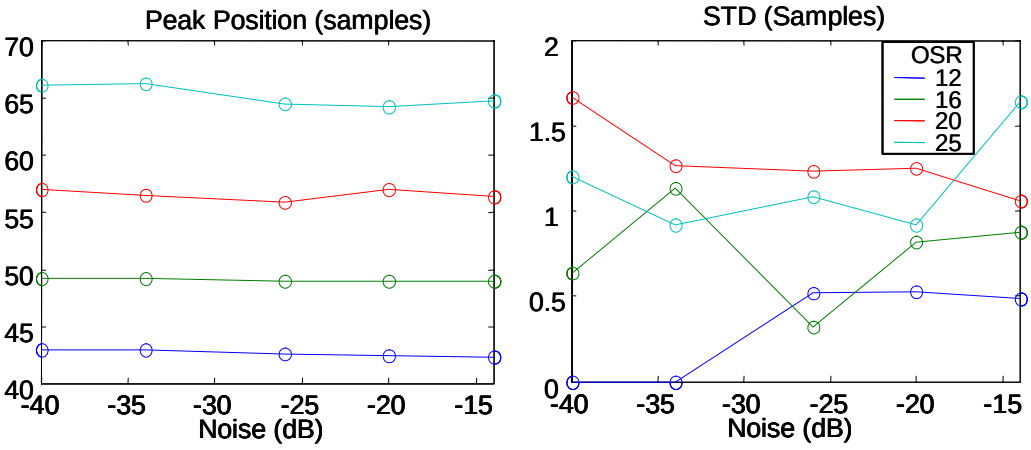

Figure 7: Variation of the signal peak position with respect to noise and oversampling ratio. Right hand: mean value, left hand: standard deviation of 100 measurement simulations

However, this error can be corrected for a given sampling frequency and low pass filter. More important is that the noise practically does not affect to the measurements. On the other hand, the standard deviation presents variations that grow with the sampling frequency from 0.5 to 2 samples. The error in the measurements corresponding to a sample is: $\Delta R = v_M / 2 f_S$, and considering v_M=1.5mm/µs, the standard deviation of the measurements

is around 0.05mm, which is less than 0.1%. Therefore, we can conclude that, with respect the radius measurement, all sampling frequencies produce good results independently of the noise content.

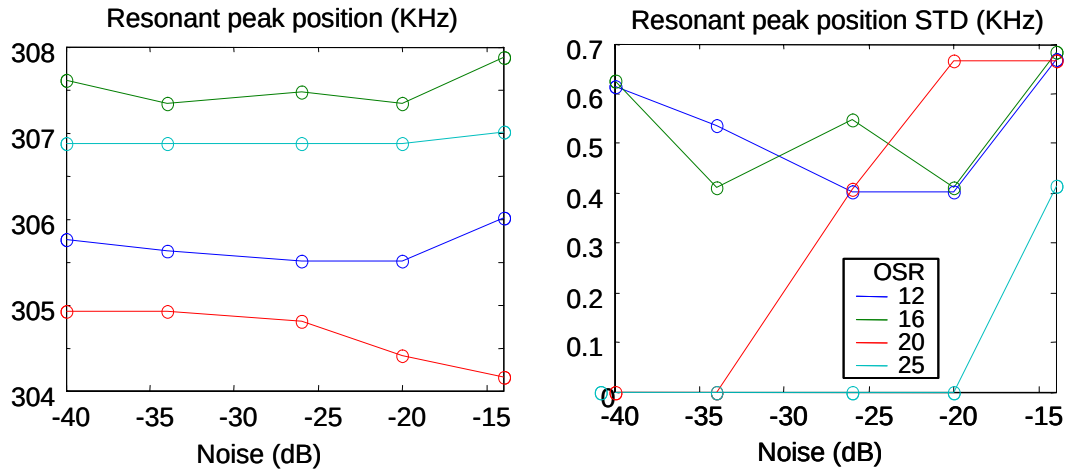

Figure 8: Variation of the resonant peak position with respect to noise and oversampling ratio. Right hand: mean value, left hand: standard deviation of 100 measurement simulations

2.2.3. Position of the resonant peak in the group delay

The position of the resonant peak in the group delay gives information of the casing thickness (equation 7). Figure 8 shows a low dependence of this parameter with respect to noise, and the error for all OSRs is within 4 KHz (1.3%). The standard deviation is in all cases very small (in the order of 0.4%).

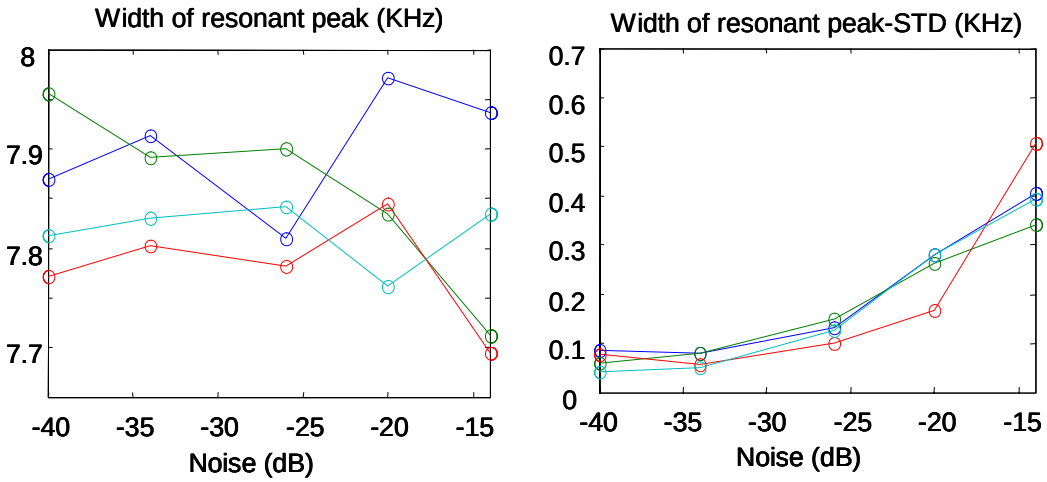

Figure 9: Variation of the width of resonant peak with respect to noise and oversampling ratio. Right hand: mean value, left hand: standard deviation of 100 measurement simulations

2.2.4. Width of the resonant peak in the group delay

The width of the resonant peak in the group delay is a measurement of the cement impedance. For the parameters of Figure 8 (10mm thick casing and Z_C=5Mrayls), the width

of the group delay resonant peak is around 7.8 KHz, and presents a slight variation of 0.3 KHz (4%) depending on the sampling frequency and noise. The standard deviation is low and constant (1%) for all OSRs when the noise level is below -25dB, but it grows to 0.4 KHz (6%) for higher noise.
From these results, it seems that an oversampling ratio OSR=12 is enough for the measurements. This means that, if we consider tubes of 5mm thick as a limit for the inspection system, the corresponding resonance frequency is 0.66 KHz, and the minimum sampling frequency for the array system is 25MHz. Therefore, all the system components should be designed for supporting the heat produced with a clock system of 25 MHz. This could be a limit for non destructive testing systems in fluid filled oil wells.

Conclusions

A simulation system has been presented for the design of an 2D cylindrical array system for non-destructive testing of tubes in harsh environments. The design is conditioned by the high number of channels and the use of SD modulators (which require high sampling frequencies) for AD conversion, both causing a great cost of energy. Our goal has been then to minimize the sampling frequency but obtaining good measurements. We have shown that the averaging effect of the array beamforming produce a great reduction of the quatization noise (beside other noise added to the signals) and therefore a low oversampling ratio (OSR) can be used holding good results in the measurements.

Acknowledgements

Work performed in the framework of EC GROW project PharusIT (G1RD-CT-2002-000689). The authors thank Børge Strand for performing SD ToolBox.

References

[1] A.J. Hayman , “Ultrasonic Properties of Oil- Well Drilling Muds”, Proceedings IEEE Ultrasonic Symposium, 1989, pp. 327-332
[2] A.J. Hayman et al. “High resolution cementation and corrosion imaging by ultrasound”, SPLWA 32th Annual Symposium, June 1991, Middland, Texas, USA
[3] A.J. Hayman et al., « Improved borehole imaging in ultrasonics », Society of Petroleum Engineers, Inc. 1995, pp. 1-14
[4] S.R. Freeman, “An oversampled ultrasound beamformer for low power portable scanners”, Ph. Dr Thesis, University of Michigan, 1998.
[5] S.R. Freeman, et al. ”Delta-sigma oversampled ultrasound beamformer with dynamic delays”, IEEE Trans UFFC, vol 46 (2), 1999, pp. 320-332.